

Monodictyochromes A and B, Dimeric Xanthone Derivatives from the Marine Algalicolous Fungus *Monodictys putredinis*

Alexander Pontius,[†] Anja Krick,[†] Ronak Mesry,[†] Stefan Kehraus,[†] Silke E. Foegen,[‡] Michael Müller,[‡] Karin Klimo,[§] Clarissa Gerhäuser,[§] and Gabriele M. König^{*,†}

Institute for Pharmaceutical Biology, University of Bonn, Nussallee 6, 53115 Bonn, Germany, Institute of Pharmaceutical Sciences, Albert-Ludwigs-University Freiburg, Albertstrasse 25, 79104 Freiburg, Germany, and Department of Toxicology and Cancer Risk Factors, DKFZ-German Cancer Research Center, Im Neuenheimer Feld 280, D-69120 Heidelberg, Germany

Received June 30, 2008

Investigations of the marine-derived fungus *Monodictys putredinis* led to the isolation of two novel dimeric chromanones (**1**, **2**) that consist of two uniquely modified xanthone-derived units. The structures were elucidated by extensive spectroscopic measurements including NOE experiments and CD analysis to deduce the configuration. The compounds (**1**, **2**) were examined for their cancer chemopreventive potential and shown to inhibit cytochrome P450 1A activity with IC₅₀ values of 5.3 and 7.5 μM, respectively. In addition, both compounds displayed moderate activity as inducers of NAD(P)H:quinone reductase (QR) in cultured mouse Hepa 1c1c7 cells, with CD values (concentration required to double the specific activity of QR) of 22.1 and 24.8 μM, respectively. Compound **1** was slightly less potent than compound **2** in inhibiting aromatase activity, with IC₅₀ values of 24.4 and 16.5 μM.

Xanthenes have been described as so-called “privileged structures”,¹ since this large group of natural products revealed a broad spectrum of pharmacological activities. They influence several inflammatory mediators such as the arachidonic acid cascade,^{2,3} enzymes such as various kinases and proteases,⁴ and receptors such as monoamine oxidase B (MAO-B).⁵ Moreover, they exhibit antimicrobial activity against a large number of human pathogenic organisms.⁶ Consequently, xanthonic molecules are a distinguished structural type, of value to the discovery of new pharmaceutically interesting compounds.

Recently, we have identified novel monomeric xanthone derivatives from *Monodictys putredinis* with cancer chemopreventive potential.⁷ In continuation of these studies, we here present two new dimeric xanthone-derived compounds that were also evaluated for their *in vitro* ability to prevent cancer. Chemoprevention in fighting carcinogenesis involves the use of nutrients and/or pharmaceuticals to block, inhibit, or reverse tumor development at various steps during the initiation, promotion, or progression phase of carcinogenesis.⁸ Phase 1 enzymes are responsible for the metabolic functionalization of xenobiotics, enabling their elimination as conjugates by phase 2 enzymes. While oxidation catalyzed by cytochrome P450 enzymes is a common phase 1 process, the biochemical activation of xenobiotics can also risk the danger of generating more potent carcinogens. Accordingly, one target for chemoprevention is the inhibition of elevated levels of cytochrome P450 isoforms such as CYP1A enzymes, which are often induced by carcinogens such as the planar aromatic hydrocarbon benzo[*a*]pyrene. Such aromatic compounds have been shown to play a role in the development of lung and breast cancer.⁹ Phase 2 enzymes decrease circulating levels of carcinogenic agents by accelerating their renal or biliar elimination. In particular, NAD(P)H:quinone reductase (QR) contributes to the detoxification of quinones by catalyzing a two-electron reduction to hydroquinones, which are subsequently eliminated as hydrophilic macromolecules.¹⁰ Accordingly, the aim of a cancer chemopreventive strategy can include the inhibition of phase 1 enzymes accompanied by an increased phase 2 metabolism, as exemplified for the chemopreventive activity of flavonoids.¹¹

Results and Discussion

The uncommon fungus *Monodictys putredinis*, isolated from an unidentified green alga collected in Tenerife, Spain, was investigated for its secondary metabolites after cultivation on a solid biomalt medium. Vacuum liquid chromatographic (VLC) and HPLC separation steps resulted in the isolation of two compounds (**1**, **2**), each consisting of two unusually modified xanthone subunits. Compounds **1** and **2** differ concerning the site of connection of subunits I and II.

The molecular formula of compound **1** was shown to be C₃₀H₃₀O₁₁ on the basis of HREIMS, which included 16 degrees of unsaturation. UV-absorption maxima at λ_{max} 206, 277, and 357 nm suggested an extended, mesomerically stabilized aromatic system. Due to the molecular formula and 29 protons evident from ¹H NMR, one proton was likely present as an aliphatic hydroxyl group. Two downfield shifted singlet proton resonances (δ_H 11.94, OH-1'; δ_H 11.69, OH-1) resulted from chelated hydroxyl protons bonded to adjacent carbonyl functions. A characteristic feature of the ¹³C NMR spectrum was the apparent “twinning” of each carbon resonance. This indicated a dimeric structure with almost the same substitution pattern for each subunit. Thus, the molecule contained 30 carbon atoms attributable to four methyl, four methylene, and seven methine groups and 15 quaternary carbons, as indicated by a DEPT spectrum. Four downfield shifted carbon resonances were part of two carbonyl functionalities adjacent to phenolic moieties (δ_C 198.9, C-9'; δ_C 197.8, C-9) and two further carboxylic groups (δ_C 176.1, C-8'; δ_C 175.3, C-8). The backbone of each subunit was determined to be a chromanone heterocycle. In subunit I, the connection of the phenyl ring to the corresponding pyran-4-one ring was proven by ¹H–¹³C HMBC correlations of H-8a'α to C-9a', H-3' to C-9a', and H-4' to C-9' (see Figure S1, Table 2). Due to ¹H NMR resonances for two *ortho*-coupled aromatic protons (δ_H 7.18, H-3'; δ_H 6.48, H-4'), only one possible site for substitution remained on the benzene ring. The key HMBC coupling between OH-1' and the quaternary carbon C-2' defined the position of the aromatic protons at C-3' and C-4' in subunit I and identified C-2' as the further substituted carbon. The ¹H–¹H COSY spectrum allowed the development of a saturated spin system between H-5', H-6', H₃-13', and H₂-7'. Long-range HMBC correlations between H₂-7' and C-8' and between H-5' and C-8' indicated the presence of a methylated γ-lactone ring. The connection of the lactone ring to C-10a' was deduced from HMBC cross-peaks between H-5' and

* To whom correspondence should be addressed. Tel: +49228733747. Fax: +49228733250. E-mail: g.koenig@uni-bonn.de.

[†] University of Bonn.

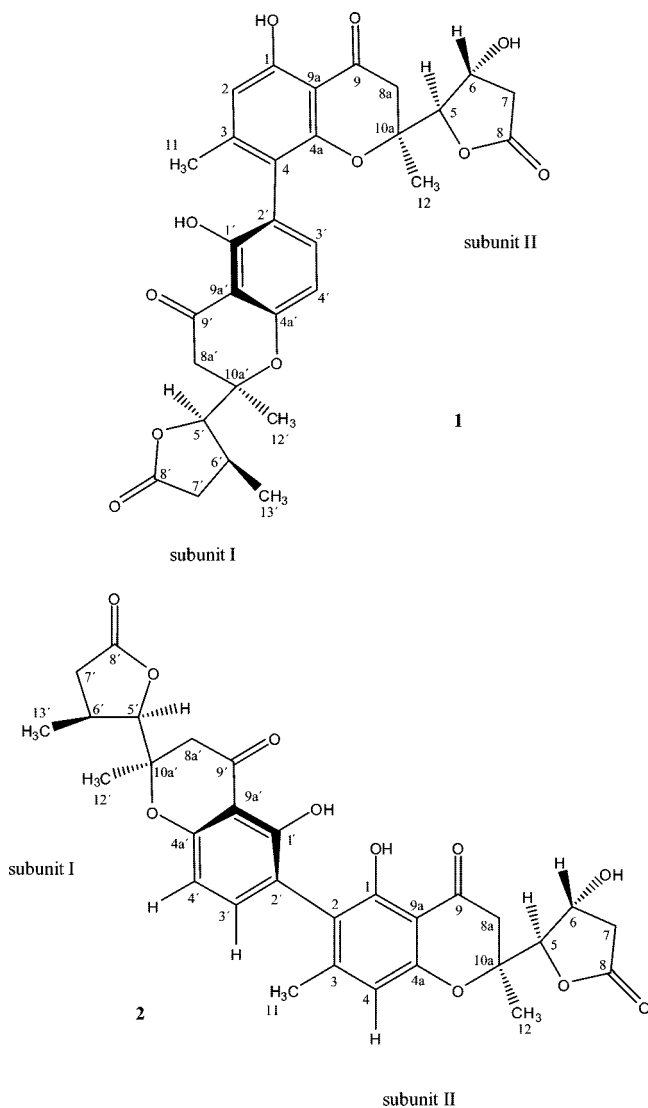
[‡] University of Freiburg.

[§] DKFZ-German Cancer Research Center.

Table 1. Influence on Carcinogen-Metabolizing Enzymes and Aromatase Activity

compound	CYP1A inhibition IC ₅₀ (μM) ^a	NAD(P)H: quinone reductase induction (QR)		aromatase inhibition IC ₅₀ (μM) ^a
		CD (μM) ^b	IC ₅₀ (μM) ^a	
1	5.3 ± 1.1	22.1 ± 1.0	>50	24.4 ± 4.8
2	7.5 ± 0.9	24.8 ± 2.6	>50	16.5 ± 1.8

^a IC₅₀: half-maximal inhibitory concentration. Mean ± standard deviation, *n* = 3. ^b CD: concentration required to double the specific activity of QR.



C-8a'. The remaining residue at the quaternary carbon C-10a' was identified as a methyl group (δ_C 19.3, C-12') showing HMBC interactions to C-8a' and C-10a'.

The chromanone structure of subunit II was established from HMBC correlations of H-8a β to C-9a, H-2 to C-4a, and H-2 to C-9. The ¹H NMR resonance for one singlet aromatic proton (δ_H 6.45, H-2) showed differences in the substitution pattern of the benzene moieties in subunits I and II. The ¹H-¹H COSY experiment revealed a small coupling between the *ortho*-positioned residues H-2 and CH₃-11. The key HMBC coupling between OH-1 and the methine carbon CH-2 and the correlation of CH₃-11 to the quaternary carbon C-4 defined the substitution pattern of the benzene moiety of subunit II and clarified that a further substituent had to be placed at C-4. The ¹H-¹H COSY experiment displayed an aliphatic spin system from H-5 through H₂-7 and was part of a second γ -lactone shown by HMBC correlations between H₂-7 and

C-8 and between H-5 and C-8. Different from subunit I, this lactone ring was substituted with a hydroxyl group instead of a methyl residue at CH-6 (δ_C 68.2). From corresponding HMBC correlations, such as found for subunit I, the γ -lactone ring and the methyl group C-12 (δ_C 19.6) were considered to be bonded at C-10a. In conclusion, the subunits were connected asymmetrically via the benzene carbons C-2' and C-4, forming a rotationally hindered biaryl axis. HMBC correlation of H-3' and C-4 supported this architectural arrangement.

Compound **1** has three chiral centers in each subunit, and the relative configurations at C-5', C-6', C-10a', and C-5, C-6, C-10a, respectively, were deduced from the magnitude of ¹H-¹H coupling constants and selective NOE experiments. In subunit I the proton resonance of H-5' appeared as a doublet with $J_{5',6'} = 5.2$ Hz that required *cis* configuration of the protons H-5' and H-6' on the alicyclic moiety. NOE enhancements observed for the ¹H NMR resonances of H-8a α' and CH₃-12' upon irradiation of the H-5' resonance indicated that the methylene proton H-8a α' , the methyl group CH₃-12', and H-5' were located on the same side of the molecule and that proton 8a α' and the methyl group were in the pseudoaxial position (see Figure 1). Accordingly, as expected for bulkier moieties, the lactone ring was in a pseudoequatorial orientation. This was confirmed by a further NOE correlation between the lactone methyl group CH₃-13' and chromanone methyl group CH₃-12' (see Table 2).

In subunit II the proton resonance of H-5 appeared as a doublet with $J_{5,6} = 1.5$ Hz, while the signal of H-6 revealed three couplings [H-7 α ($J_{6,7\alpha} = 1.5$ Hz, *trans*), H-7 β ($J_{6,7\beta} = 6.7$ Hz, *cis*), and H-5 ($J_{6,5} = 1.5$ Hz, *trans*)]. Thus, H-5 and H-6 possessed a *trans* configuration on the alicyclic lactone. NOE enhancements of H-8a α and CH₃-12 were observed upon irradiation of the resonance for H-5 and suggested the same spatial orientation of the methyl group CH₃-12, H-5, and H-8a α , leading to a pseudoequatorial position for the lactone ring (see Figure 1). Taking the results of proton coupling constant analysis and NOE data into account, the relative configuration of the chiral centers was deduced independently for each subunit as 5'R*, 6'S*, 10a'R* and 5R*, 6R*, 10aS*, respectively.

Compound **1** has a chiral axis between C-2' and C-4 that was analyzed using CD spectroscopy. The CD spectrum of **1** was compared with that of the similarly substituted reference molecule (*P*)-orsellinic acid camphanate (**3**), whose absolute configuration has been established by X-ray crystallographic studies.¹² The nearly congruent CD curves with the same sign for induced Cotton effects for the aromatic systems suggested the *P*-absolute configuration for compound **1** (see Figure 2). Furthermore, an NOE correlation between CH-3' and CH₃-12 allowed, in conjunction with the *P*-configuration of the chiral axis, deduction of the absolute configuration of the chiral carbons of subunit II as 5R, 6R, 10aS (see Figure 4). No significant NOE correlation was found, however, to assign the absolute configuration of the chiral centers in subunit I. We propose the trivial name monodictyochrome A for compound **1**.

Compound **2** possessed the same molecular formula as compound **1**, as deduced from HREIMS measurements, and showed very similar NMR data. The main differences as observed in the HMBC spectra were the correlations of the hydroxyl group proton OH-1 (δ_H 11.91), the singlet aromatic proton H-4 (δ_H 6.41), and the methyl group CH₃-11 (δ_H 2.07) of subunit II (see Figure S1, Table 3). Hydroxyl-1 showed only HMBC cross-peaks to the quaternary carbons C-2 and C-9a. Combined with the HMBC interactions of H-4 to C-2 and of CH₃-11 to C-1, the linkage of the subunits had to be between C-2' and C-2. The HMBC correlation of H-3' and C-2 sustained this deduction. All other data including NOEs and the magnitude of ¹H-¹H coupling constants were close to identical to those for compound **1**, indicating the same relative configuration of the chiral centers (see Figure 1). Thus, compounds **1** and **2** were regioisomers. However, compound **2** showed a mirror-inverted CD

Table 2. NMR Data for Compound 1

atom no.	$^{13}\text{C}^{a,c,f}$ (δ in ppm)	$^1\text{H}^{b,c}$ (δ ppm, mult., J in Hz)	COSY a,d	HMBC a,e	selective NOE b,d
1'	159.6 (C)				
2'	116.4 (C)				
3'	141.7 (CH)	7.18 (d, 8.5)	4'	1', 4a', 9a', 4	4', 11, 12
4'	109.3 (CH)	6.48 (d, 8.5)	3'	2', 4a', 9', 9a'	3'
4a'	159.7 (C)				
5'	89.8 (CH)	4.35 (d, 5.2)	6', 7' α/β , 13'	6', 8', 8a', 12', 13'	8a' α , 8a' β^h , 12', 13'
6'	30.8 (CH)	2.91 (m)	5', 7', 13'	10a'	7' α
7'	36.9 (CH ₂)	2.91 (H β m) 2.31 (H α m)	6', 7' α , 13' 6', 7' β , 13'	5', 6', 8' 5', 6', 8'	6', 7' β , 13'
8'	176.1 (C)				
8a'	43.4 (CH ₂)	3.23 (H β d, 17.4) 2.80 (H α d, 17.4)	8a' α , 12' 8a' β	5', 9', 10a', 12' 9', 9a', 12'	8a' α 8a' β , 12'
9'	198.9 (C)				
9a'	108.0 (C)				
10a'	82.9 (C)				
12'	19.3 (CH ₃)	1.56 (s)	8a' β	5', 8a', 10a'	5', 6', 8a' α , 13'
13'	20.5 (CH ₃)	1.29 (d, 6.7)	5', 6', 7' α/β	5', 6', 7'	5', 8a' β , 7' α , 12'
OH-1'		11.94 (s)		1', 2', 3', 9a'	
1	161.8 (C)				
2	110.7 (CH)	6.45 (br s)	11	1, 4, 4a, 9, 9a, 11	11
3	150.9 (C)				
4	117.2 (C)				
4a	156.7 (C)				
5	91.9 (CH)	4.30 (d, 1.5)	6	4a, 6, 7, 8, 8a, 10a	8a α , 8a β^h , 12
6	68.2 (CH)	4.77 (dt, 6.7, 1.5)	5, 7 α/β	5, 8, 10a	8a β
7	38.0 (CH ₂)	2.36 (H β dd) 2.10 (H α dd)	6, 7 α 6, 7 β	6, 8 5, 6, 8	6, 7 α
8	175.3 (C)				
8a	42.4 (CH ₂)	3.31 (H β d, 17.4) 2.64 (H α d, 17.4)	8a α , 12 8a β	5, 9, 10a, 12 9, 9a, 12	6, 8a α 5, 8a β , 12
9	197.8 (C)				
9a	106.3 (C)				
10a	81.7 (C)				
11	21.2 (CH ₃)	2.06 (br s)	2	2, 3, 4	2, 7 β
12	19.6 (CH ₃)	1.42 (s)	8a β	5, 6, 8a, 10a	5, 8a α , 3'
OH-1		11.69 (s)		1, 2, 4a, 9a	

^a Acetone- d_6 , 300/75.5 MHz. ^b Acetone- d_6 , 500/125.7 MHz. ^c Assignments are based on extensive 1D and 2D NMR measurements (HMBC, HSQC, COSY). ^d Numbers refer to proton resonances. ^e Numbers refer to carbon resonances. ^f Implied multiplicities determined by DEPT. ^h Weak correlation.

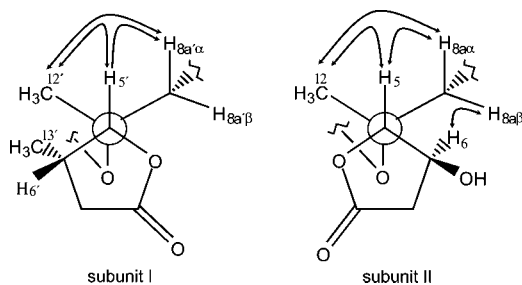


Figure 1. Important selective gradient NOEs (arrows) of subunits I and II depicted as Newman projections (along the 5'–10a'/5–10a axis, respectively) for compounds **1** and **2**.

spectrum that corresponded to the recorded curve of the *M*-atropisomer of an orsellinic camphanate reference (**4**) (see Figure 3). Accordingly, compound **2** was considered to have a chiral axis with *M*-absolute configuration. Because no NOE correlations between the subunits were detected, the absolute configuration of the chiral centers could not be deduced. We propose the trivial name monodictyochrome B for compound **2**.

Both compounds isolated during this study have a chromanone basic structure, most probably derived from xanthone precursors. The biosynthetic pathway from an octaketide starter via an anthraquinone skeleton to a xanthone heterocycle is already amply described, and the position of the methyl group at either C-3 or C-6' in the subunits of **1** and **2** can be seen as the result of the two possible cleavage sites in the anthraquinone skeleton (see Figure S2).^{13,14} The rearrangement of one of the outer rings of this scaffold, however, to the so-called ergochrome F unit (related to ergoxan-

thin)¹⁵ is described to date only for a few fungal-derived compounds, such as xanthoquinodins A3 and B3,¹⁶ chaetomanone,¹⁷ and the lachnones 3, 4, and 5¹⁸ (see Figure S5). Each of these compounds, apart from the lachnones, has a dimeric nature with one of the subunits being anthraquinone- and the other xanthone-related. In compounds **1** and **2** two xanthone-derived units are connected, probably as the result of a regioselective phenol oxidative coupling involving two activated sites of the aromatic moieties in subunits I and II. Moreover, the connection of both subunits is most probably stereoselectively controlled since CD spectroscopy unequivocally showed the presence of two atropisomers [monodictyochrome A is the *P*-stereoisomer and monodictyochrome B the *M*-stereoisomer].¹⁹

On the basis of our previous findings with xanthone monomers,⁷ both compounds were evaluated for their potential to inhibit the phase I enzyme CYP1A and to induce the phase II enzyme NAD(P)H:quinone reductase (QR). As shown in Figure 5, both compounds dose-dependently inhibited β -naphthoflavone-induced CYP1A enzymatic activity of H4IIE cell homogenates with half-maximal inhibitory concentrations (IC₅₀) of 5.3 ± 1.1 and $7.5 \pm 0.9 \mu\text{M}$ (see Table 1, Figure 5).

Concomitantly, both compounds also induced NAD(P)H:quinone reductase (QR) activity in Hepa 1c1c7 murine hepatoma cell culture in a dose-dependent manner (see Figure 6). CD values were in the range of 22.1 ± 1.0 and $24.8 \pm 2.6 \mu\text{M}$, without cytotoxic effects at concentrations up to $50 \mu\text{M}$ (see Table 1). Concentrations for QR induction were, however, about 100-fold higher than those required of the positive control, sulforaphane, derived from broccoli. Sulforaphane has been described as the most potent natural phase 2 inducer identified so far.²⁰

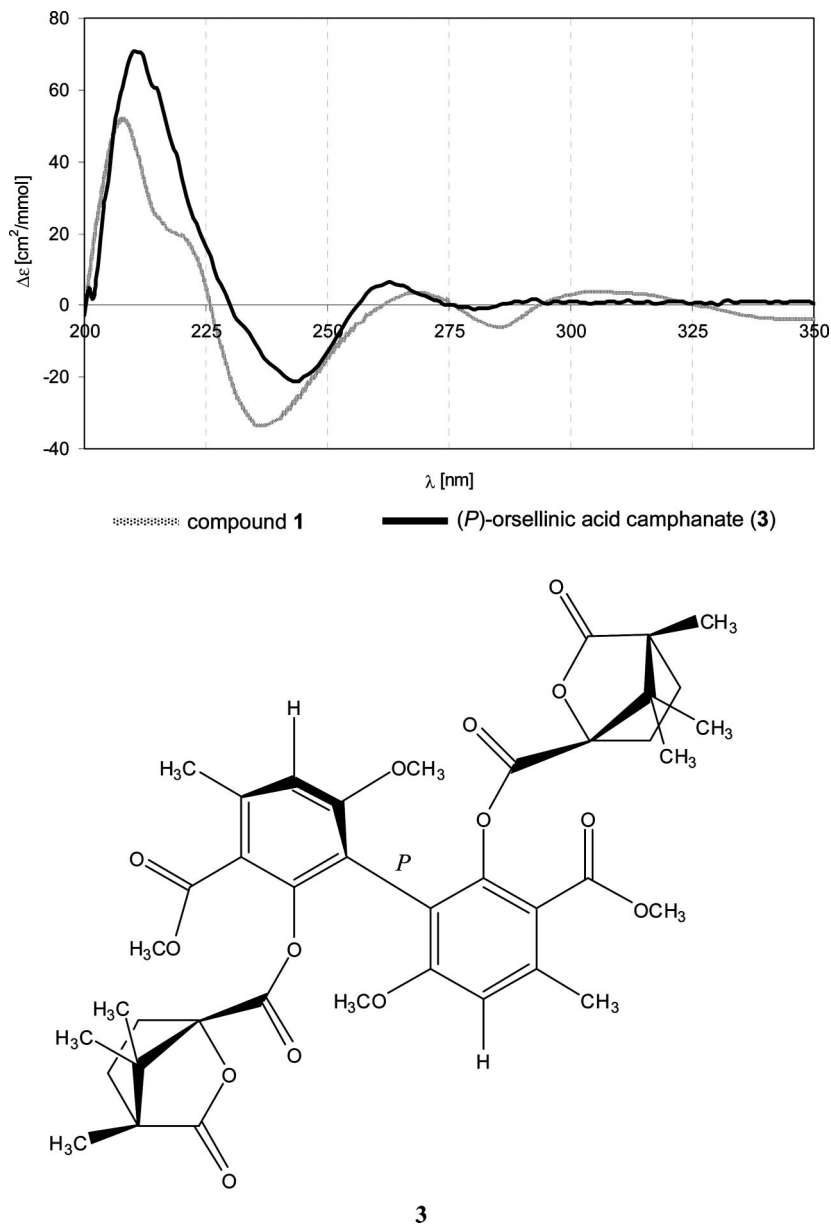


Figure 2. CD spectra of compound **1** and the reference (*P*)-orsellinic acid camphanate (**3**) in MeOH.

Reactive oxygen species play a role in the initiation and promotion phase of carcinogenesis. Using the stable radical 1,1-diphenyl-2-picrylhydrazyl (DPPH),²² we were not able to demonstrate radical-scavenging potential at concentrations up to 250 μM . We also investigated antioxidant potential by scavenging of superoxide anion radicals generated by oxidation of hypoxanthine to uric acid by xanthine oxidase.²² Neither compound showed any activity at concentrations up to 50 μM . Also, we determined oxygen radical absorbance capacity (ORAC), using 2,2-azobis(2-amidinopropane) dihydrochloride (AAPH) as a peroxy-radical generator.²² At a concentration of 1 μM , both compounds were less potent in scavenging peroxy radicals than the water-soluble vitamin E analogue trolox used as a reference compound.

Finally, we also investigated the potential of both compounds to inhibit tumor promotion using cyclooxygenase-1 (COX-1) and aromatase enzymatic activities as marker systems.^{22,23} Both compounds were unable to inhibit COX-1 activity more than 50% at a concentration of 100 μM . Compound **2** was slightly more potent than compound **1** in inhibiting activity of aromatase, with an IC_{50} value of $16.5 \pm 1.8 \mu\text{M}$ (see Table 1). Dose-dependent inhibition is shown in Figure S6.

In conclusion, monodictyochromes A and B (**1**, **2**) may contribute to the prevention of carcinogenesis by inhibition of cytochrome P450 enzymes such as CYP1A, involved in carcinogen activation, and CYP19 (aromatase), essential for estrogen biosynthesis. In addition, both compounds moderately induced QR activity as an indication of enhanced carcinogen detoxification.

Experimental Section

General Experimental Procedures. Optical rotations were measured on a JASCO DIP 140 polarimeter. UV and IR spectra were obtained employing Perkin-Elmer Lambda 40 and Perkin-Elmer Spectrum BX instruments, respectively. CD spectra were recorded at room temperature on a Jasco J-810 spectrophotometer in 1 cm cuvettes. ^1H (1D, 2D COSY) and ^{13}C (1D, DEPT 135, 2D HSQC, 2D HMBC) NMR spectra were recorded on Bruker Avance 500 DRX and Bruker Avance 300 DPX spectrometers in acetone- d_6 . Spectra were referenced to residual solvent signals with resonances at $\delta_{\text{H/C}}$ 2.04/28.9 (acetone- d_6). HREIMS were recorded on a Finnigan-MAT 95 spectrometer. HPLC-MS measurements were recorded employing an Agilent 1100 Series HPLC including DAD, with a reversed-phase C_{18} column (Macherey-Nagel Nucleodur 100, 125 mm \times 2 mm, 5 μM) and gradient elution (from MeOH-H $_2$ O, 10:90, in 20 min to 100% MeOH, then isocratic for 10 min), coupled with an API 2000, Triple Quadrupole, LC/MS/MS,

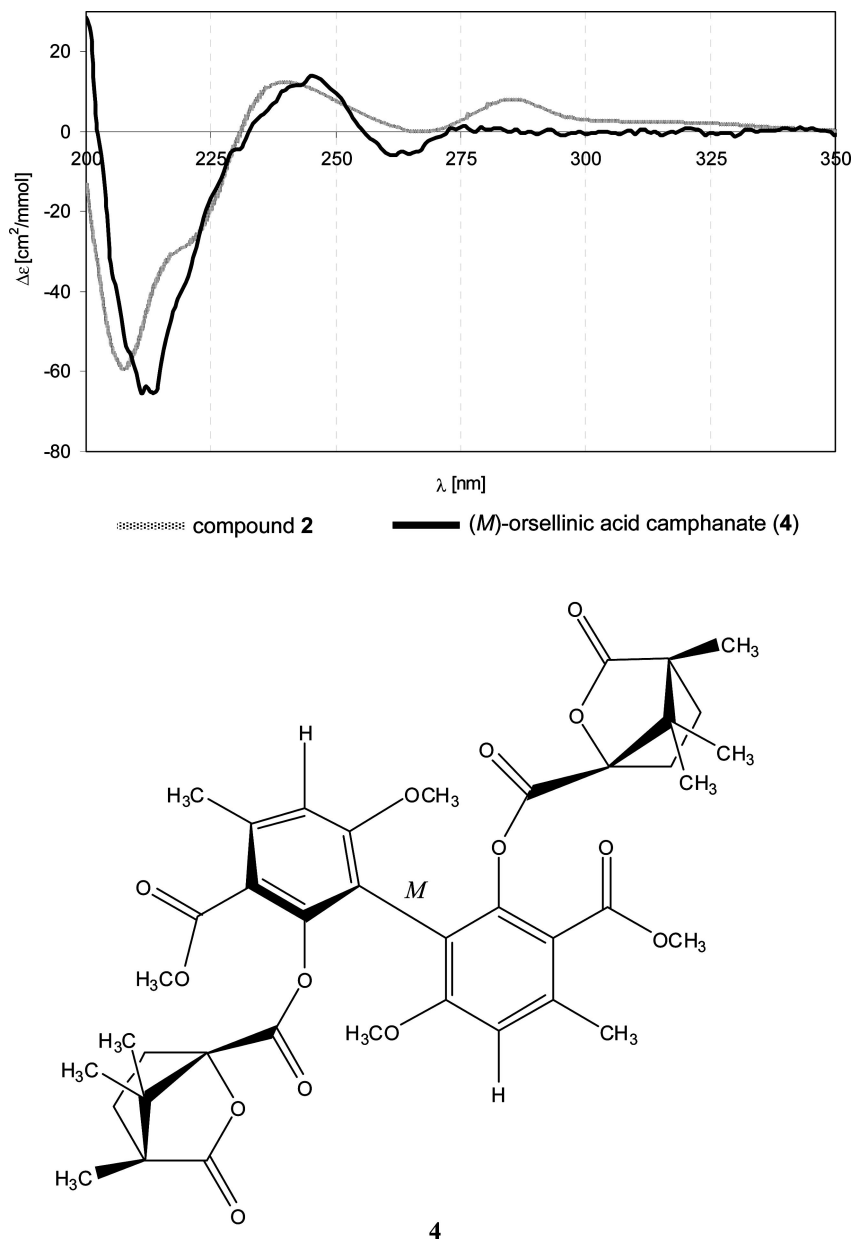


Figure 3. CD spectra of compound **2** and the reference (*M*)-orsellinic acid camphanate (**4**) in MeOH.

Applied Biosystems/MDS Sciex and ESI source. Preparative HPLC was carried out using a Merck-Hitachi system consisting of a L-6200A pump, a L-4500 photodiode array detector, and a D-6000 interface or a Waters system with 515 HPLC pump and a Knauer K-2300 differential refractometer as detector.

Origin of the Algal Sample. The fresh algal sample was collected in September 1995 in Tenerife, Spain. Until examination the sample was stored in sterile artificial seawater [ASW (g/L): KBr (0.1), NaCl (23.48), $\text{MgCl}_2 \times \text{H}_2\text{O}$ (10.61), $\text{CaCl}_2 \times 2 \text{H}_2\text{O}$ (1.47), KCl (0.66), $\text{SrCl}_2 \times 6 \text{H}_2\text{O}$ (0.04), Na_2SO_4 (3.92), NaHCO_3 (0.19), H_3BO_3 (0.03)]. Algal samples were rinsed three times with sterile H_2O . After surface sterilization with 70% EtOH for 15 s the alga was rinsed in sterile ASW. The alga was aseptically cut into small pieces and placed on agar plates containing isolation medium: 15 g/L agar (Fluka Chemie GmbH, Buchs, Switzerland), ASW 800 mL/L, glucose 1 g/L, peptone from soymeal 0.5 g/L, yeast extract 0.1 g/L, benzyl penicillin 250 mg/L, and streptomycin sulfate 250 mg/L. A fungus found to grow out of the algal tissue was separated on biomalt medium (biomalt 20 g/L, agar 10 g/L, ASW 1000 mL/L) until the culture was pure. The fungal strain 195 15 I was identified as *Monodictys putredinis* (Wallroth) S. Hughes 1958 by Dr. R. A. Samson, Centralbureau voor Schimmelcultures, Utrecht, The Netherlands.

Cultivation. The fungal strain *M. putredinis* was cultivated on 5 L (20 Fernbach flasks) of solid biomalt medium containing 50 g/L biomalt (Villa Natura Gesundheitsprodukte GmbH, Kirn, Germany), 0.1 g/L yeast extract, and 15 g/L agar at room temperature for 4 months. Each Fernbach flask was inoculated with a piece of fungal biomass (1 cm^2) dissolved in 10 mL of sterile H_2O .

Extraction and Isolation. Fungal biomass and media were diluted with H_2O (100 mL/L) and homogenized using an Ultra-Turrax apparatus. Exhaustive extraction with 21 L of EtOAc in three steps yielded 5.3 g of brown, oily extract. This was fractionated by normal-phase VLC (silica gel 60, 0.063–0.200 mm) using gradient elution from petroleum ether, EtOAc, and acetone to MeOH, to yield 11 fractions. Fraction 4 showed interesting ^1H NMR spectra and antimicrobial activity; the LC-MS fingerprint chromatogram contained several interesting peaks. Fractions 9 and 11 were purified under the same conditions by RP18 HPLC (Knauer C_{18} Eurospher-100 column, 250 \times 8 mm, 5 μM , MeOH/ H_2O , 7:3, 2 mL/min). Fraction 4.9.2 yielded 6.0 mg of compound **1**, and fraction 4.11.3 yielded 10.0 mg of compound **2**.

Monodictyochromone A (1): yellow solid (6.0 mg, 2.4 mg/L); $[\alpha]_D^{24} -67$ (c 0.42 CHCl_3); UV (MeOH) λ_{max} (log ϵ) 206 (4.46), 277 (4.20), 357 (3.75) nm; CD (c 0.018, MeOH) λ ($\Delta\epsilon$) 208 (+51.6), 237

Table 3. NMR Data for Compound 2

atom no.	$^{13}\text{C}^{a,c,f}$ (δ in ppm)	$^1\text{H}^{b,c}$ (δ ppm, mult., J in Hz)	COSY a,d	HMBC a,e	selective NOE b,d
1'	160.1 (C)				
2'	116.6 (C)				
3'	142.0 (CH)	7.31 (d, 8.5)	4'	1', 4', 2	4', 11
4'	108.3 (CH)	6.53 (d, 8.5)	3'	2', 4a', 9', 9a'	3', 13'
4a'	159.5 (C)				
5'	89.4 (CH)	4.32 (d, 4.9)	6', 7' α , 13'	6', 7', 8', 8a', 12', 13'	8a' α , 8a' β^h , 12', 13'
6'	30.8 (CH)	2.93 (m)	5', 7', 13'		
7'	36.9 (CH ₂)	2.88 (H β m) 2.26 (H α dd, 5.8, 17.7)	6', 7' α , 13' 6', 7' β , 13'	6', 8' 5', 6', 8'	7' β , 13'
8'	176.1 (C)				
8a'	43.4 (CH ₂)	3.24 (H β d, 16.8) 2.82 (H α d, 16.8)	8a' α , 12' 8a' β	5', 9', 10 α' 5', 9', 9 α' , 10 α'	8a' α 5', 7' α , 8a' β , 12'
9'	198.6 (C)				
9a'	108.1 (C)				
10a'	82.5 (C)				
12'	19.8 (CH ₃)	1.50 (s)	8a' β	5', 8a', 10a'	5', 8a' α
13'	20.5 (CH ₃)	1.28 (d, 6.5)	6', 7'	5', 6', 7'	
OH-1'		11.97 (s)		1', 2', 9a'	11
1	160.4 (C)				
2	118.0 (C)				
3	151.0 (C)				
4	109.5 (CH)	6.41 (br s)	11	2, 4a, 9, 9a, 11	11
4a	158.6 (C)				
5	91.6 (CH)	4.46 (d, 1.8)	6	6, 8, 8a, 10a, 12	8a α , 8a β^h , 12
6	68.0 (CH)	4.98 (br d, 6.7)	5, 7	8	8a β
7	38.7 (CH ₂)	3.03 (H β dd, 6.7, 17.7) 2.48 (H α dd, 2.5, 17.7)	6, 7 α 6, 7 β	8 6, 8	7 α 7 β
8	175.5 (C)				
8a	42.6 (CH ₂)	3.34 (H β d, 17.1) 2.71 (H α d, 17.1)	8a α , 12 8a β	5, 9, 10 α 9, 9 α	6 5, 8a β , 12
9	197.5 (C)				
9a	106.1 (C)				
10a	81.4 (C)				
11	21.2 (CH ₃)	2.07 (br s)	4	1, 2, 3, 4	4
12	19.5 (CH ₃)	1.50 (s)	8a β	5, 8a, 10a	5, 8a α
OH-1		11.91 (s)		1, 2, 9a	

^a Acetone- d_6 , 300/75.5 MHz. ^b Acetone- d_6 , 500/125.7 MHz. ^c Assignments are based on extensive 1D and 2D NMR measurements (HMBC, HSQC, COSY). ^d Numbers refer to proton resonances. ^e Numbers refer to carbon resonances. ^f Implied multiplicities determined by DEPT. ^h Weak correlation.

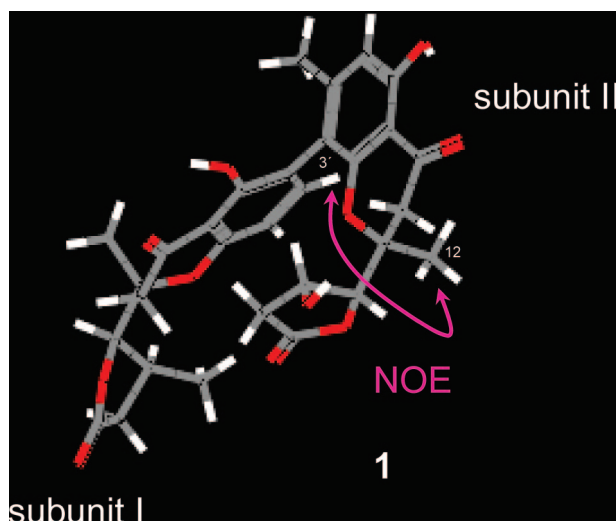


Figure 4. Selective gradient NOE correlation (purple arrow) between the two subunits of **1**. The preferred conformation was calculated using the Cerius2 4.0 (MSI) molecular modeling software package.

(−33.4), 269 (+3.8), 285 (−5.9) nm; IR (ATR) ν_{max} 3455, 1776, 1628, 746 cm^{-1} ; ^1H and ^{13}C NMR data, see Table 2; ESIMS m/z 567 [M + H] $^+$, 565 [M − H] $^-$; EIMS m/z 566 (100), 548 (20), 465 (45); HREIMS m/z 566.1791 (calcd for C₃₀H₃₀O₁₁ 566.1788).

Monodictyochromone B (2): yellow solid (10.0 mg, 4.0 mg/L); [α] $^{24}_{\text{D}}$ +74 (*c* 0.60 CHCl₃); UV (MeOH) λ_{max} (log ϵ) 205 (4.21), 279 (3.55), 359 (3.09) nm; CD (*c* 0.018, MeOH) λ ($\Delta\epsilon$): 207 (−59.0), 240 (+12.5), 267 (+0.1), 285 (+8.2) nm; IR (ATR) ν_{max} 3454, 1776, 1624,

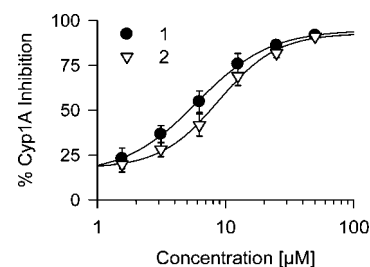


Figure 5. Dose-dependent inhibition of CYP1A enzymatic activity by compounds **1** and **2**. CYP1A activity was measured with β -naphthoflavone-induced H4IIE rat hepatoma cell homogenates by dealkylation of 3-cyano-7-ethoxycoumarin to fluorescent 3-cyano-7-hydroxycoumarin. Activities of β -naphthoflavone-induced controls were in the range of 39.4 ± 3.9 pmol/min/mg of protein ($n = 3$). α -Naphthoflavone used as a positive control inhibited CYP1A activity with an IC₅₀ value of 0.002 ± 0.001 μM .

1156, 745 cm^{-1} ; ^1H and ^{13}C NMR data, see Table 3; ESIMS m/z 567 [M + H] $^+$, 565 [M − H] $^-$, EIMS m/z 566 (40), 548 (40), 464 (100); HREIMS m/z 566.1778 (calcd for C₃₀H₃₀O₁₁ 566.1788).

Biological Assays. Compounds **1** and **2** were tested in agar diffusion assays (1 mg/mL) against the bacteria *Bacillus megaterium* and *Escherichia coli*, the fungi *Microbotryum violaceum*, *Eurotium rubrum*, and *Mycotypha microspora*, and the green microalga *Chlorella fusca* and were found to be inactive.²⁴ Cytotoxicity of the compounds was investigated using 36 tumor cell lines with no activity at concentrations of 1 and 10 $\mu\text{g/mL}$, respectively.²⁵

Determination of Potential Cancer Chemopreventive Activities. Experimental details of most test systems utilized in this study are summarized in Gerhäuser et al.^{22,26} Briefly, inhibition of CYP1A (EC 1.14.14.1) enzymatic activity and induction of QR (EC 1.6.99.2) in

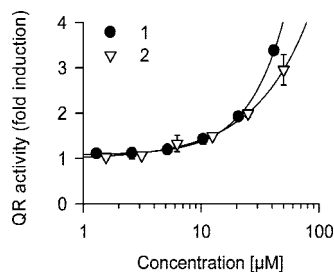


Figure 6. Induction of QR activity in Hepa 1c1c7 cell culture by compounds **1** and **2**. The specific QR activity of untreated controls was 32 ± 3 nmol/min/mg protein ($n = 4$). Sulfaphane was used as a positive control and induced QR activity with a CD value of 0.245 ± 0.012 μ M.

cultured Hepa1c1c7 cells were assayed as described by Crespi et al. (1997) and Gerhäuser et al. (1997),^{27,28} monitoring the dealkylation of 3-cyano-7-ethoxycoumarin to 3-cyano-7-hydroxycoumarin and the NADPH-dependent menadiol-mediated reduction of MTT [3-(4,5-dimethylthiazo-2-yl)-2,5-diphenyltetrazolium bromide] to a blue formazan, respectively. Inhibition of aromatase activity was estimated using human recombinant CYP19 (EC 1.14.14.1) and *O*-benzylfluorescein benzyl ester (DBF) as a substrate.²³

Acknowledgment. We thank M. Engeser and C. Sondag, Institute for Organic Chemistry, University of Bonn, Germany, for recording EIMS spectra as well as A. Maier and H.-H. Fiebig, Oncotest GmbH, Freiburg, Germany, for cytotoxicity assays. For financial support we thank the Bundesministerium für Bildung und Forschung (BMBF), research program 03F0415A.

Supporting Information Available: Important ¹H–¹H COSY and HMBC correlations, a scheme with the proposed biosynthesis, 1D and 2D NMR spectra, and related fungal metabolites of compounds **1** and **2**. This material is available free of charge via the Internet at <http://pubs.acs.org>.

References and Notes

- (1) Lesch, B.; Bräse, S. *Angew. Chem., Int. Ed.* **2004**, *43*, 115–118.
- (2) Chen, Y.-C.; Chen, K.-T. *Acta Pharmacol. Sin.* **2007**, *28*, 2027–2032.
- (3) El Sayah, M.; Cechinel-Filho, V.; Pinheiro, T. R.; Yunes, R. A.; Calixto, J. B. *Inflamm. Res.* **1999**, *48*, 218–223.
- (4) Ha, W. Y.; Wu, P. K.; Kok, T. W.; Leung, K. W.; Mak, N. K.; Yue, P. Y. K.; Ngai, S. M.; Tsai, S. N.; Wong, R. N. S. *Int. J. Biochem. Cell Biol.* **2006**, *38*, 1393–1401.

- (5) Harkcom, W. T.; Bevan, D. R. *Biochem. Biophys. Res. Commun.* **2007**, *360*, 401–406.
- (6) Pinto, M. M. M.; Sousa, M. E.; Nascimento, M. S. J. *Curr. Med. Chem.* **2005**, *12*, 2517–2538.
- (7) Krick, A.; Kehraus, S.; Gerhäuser, C.; Klimo, K.; Nieger, M.; Maier, A.; Fiebig, H.-H.; Atodiresei, I.; Raabe, G.; Fleischhauer, J.; König, G. M. *J. Nat. Prod.* **2007**, *70*, 353–360.
- (8) Sporn, M. B.; Suh, N. *Carcinogenesis* **2000**, *21*, 525–530.
- (9) Tsuji, P. A.; Walle, T. *Chem. Biol. Interact.* **2007**, *169*, 25–31.
- (10) Deng, Y.; Chin, Y.-W.; Chai, H.; Keller, W. J.; Kinghorn, A. D. *J. Nat. Prod.* **2007**, *70*, 2049–2052.
- (11) Moon, Y. J.; Wang, X.; Morris, M. E. *Toxicol. In Vitro* **2006**, *20*, 187–210.
- (12) Drochner, D.; Hüttel, W.; Bode, S. E.; M, M.; Karl, U.; Nieger, M.; Steglich, W. *Eur. J. Org. Chem.* **2007**, *11*, 1749–1758.
- (13) Steyn, P. S. *J. Environ. Pathol. Toxicol. Oncol.* **1992**, *11*, 47–59.
- (14) Bringmann, G.; Noll, T. F.; Gulder, T. A. M.; Grüne, M.; Dreyer, M.; Wilde, C.; Pankewitz, F.; Hilker, M.; Payne, G. D.; Jones, A. L.; Goodfellow, M.; Fiedler, H.-P. *Nat. Chem. Biol.* **2006**, *2*, 429–433.
- (15) Franck, B.; Flasch, H. *Fortschr. Chem. Org. Naturst.* **1973**, *30*, 151–206.
- (16) Tabata, N.; Tomoda, H.; Iwai, Y.; Omura, S. *J. Antibiot.* **1996**, *49*, 267–271.
- (17) Kanokmedhakul, S.; Kanokmedhakul, K.; Phonkerd, N.; Soyong, K.; Kongsaree, P.; Suksamrarn, A. *Planta Med.* **2002**, *9*, 834–836.
- (18) Rukachaisirikul, V.; Chantaruk, S.; Pongcharoen, W.; Isaka, M.; Lapanun, S. *J. Nat. Prod.* **2006**, *69*, 980–982.
- (19) Hüttel, W.; Müller, M. *ChemBioChem* **2007**, *8*, 521–529.
- (20) Posner, G. H.; Cho, C.-G.; Green, J. V.; Zhang, Y.; Talalay, P. *J. Med. Chem.* **1994**, *37*, 170–176.
- (21) Valko, M.; Leibfritz, D.; Moncol, J.; Cronin, M. T.; Mazur, M.; Telser, J. *Int. J. Biochem. Cell Biol.* **2007**, *39*, 44–84.
- (22) Gerhäuser, C.; Klimo, K.; Heiss, E.; Neumann, I.; Gamal-Eldeen, A.; Knauff, J.; Liu, G.-Y.; Sitthimonchai, S.; Frank, N. *Mutat. Res.* **2003**, *523–524*, 163–172.
- (23) Stresser, D. M.; Turner, S. D.; McNamara, J.; Stocker, P.; Miller, V. P.; Crespi, C. L.; Patten, C. *J. Anal. Biochem.* **2000**, *284*, 427–430.
- (24) Schulz, B.; Sucker, J.; Aust, H. J.; Krohn, K.; Ludewig, K.; Jones, P. G.; Döring, D. *Mycol. Res.* **1995**, *99*, 1007–1015.
- (25) Fiebig, H.-H.; Maier, A.; Burger, A. M. *Eur. J. Cancer* **2004**, *40*, 802–820.
- (26) Gerhäuser, C.; Alt, A.; Heiss, E.; Gamal-Eldeen, A.; Klimo, K.; Knauff, J.; Neumann, I.; Scherf, H.-R.; Frank, N.; Bartsch, H.; Becker, H. *Mol. Cancer Ther.* **2002**, *1*, 959–969.
- (27) Crespi, C. L.; Miller, V. P.; Penman, B. W. *Anal. Biochem.* **1997**, *248*, 188–190.
- (28) Gerhäuser, C.; You, M.; Liu, J.; Moriarty, R. M.; Hawthorne, M.; Mehta, R. G.; Moon, R. C.; Pezzuto, J. M. *Cancer Res.* **1997**, *57*, 272–278.

NP800392W